Thermopower simulation of a two level spinless quantum dot

Susanna Hammarberg

May 12, 2014

Supervisors: Prof. Andreas Wacker and
Olov Karlström

Division of Mathematical Physics

UNIVERSITY

Abstract

Quantum dots are interesting candidates for a broad variety of electronic components, with single electron transistors and LEDs being two examples already well on their way. In nanostructures, such as quantum dots, quantum effects greatly influence the transport. In a spin polarized quantum dot system with two energy levels, interference effects have been found to cause a strong suppression of conductance [Phys. Rev. Lett. **104**, 186804 (2010)]. In the present work, this system is further investigated with thermopower acting as probing tool. Thermopower is a measure of the voltage induced by a temperature difference, attributed to the Seebeck effect, at vanishing current. While conductance probes transport at and around the Fermi level, thermopower does so for a wider range of energies. For the system addressed in this work, thermopower is evaluated as a probing tool complementary to conduction. To simulate transport, a generalized master equation approach is used; the *second order von Neumann* approach. This method takes into account second order tunneling as well as interference effects; coherence and correlations. The simulations show that the conductance suppression manifest itself also in the thermopower and furthermore, with a more prominent signal.

Contents

Part I
Introduction and outline

1   Introduction

1.1   Transport in nanostructures

The applications of nanostructures have expanded in pace with the development of the technology. Often it is the size itself, or the properties that come with the size, that are desirable in a structure. A quantum dot (QD) confines charge carriers in all three dimensions, resulting in a 0D system. Such structures are often formed by sandwiching one type of semiconductor with another. With two different band gaps, their conduction bands will form a well when merged together. This potential well is what confines electrons and forms the QD. QDs made out of metal are also common. These QDs have much more dense energy levels, thereby they contain many more electrons[1]. Therefore, transport through QDs of metal or semiconductors has to be described differently. In this work, we are considering semiconductor QDs with only two well separated energy levels.

By connecting a QD to leads via tunneling barriers, it is possible to run a current through the device. Conducting QDs have already been used as components of electric circuits such as in single electron transistors[2] and LED's[3]. These components have the advantage that that they allow for high control over conductance properties. One is able to determine the energy of electrons that are allowed to pass through the device. A small semiconductor QD with only a few energy levels that are well separated is well suited for fundamental research. One can investigate how the transport is affected by, e.g., Coulomb repulsion or quantum effects like coherence and interference.

When two energy levels are degenerate, interference effects can play an extra role for transport. A simple system, where one can investigate this, is a two level QD coupled to leads. At degeneracy of two levels of different spin, the conductance experiences an enhancement at low temperatures. This is because a single electron in the QD and electrons in the leads form a singlet state in resonance with the Fermi energy; the *Kondo effect*[4] In Ref. [5], the authors model the rarer case of two degenerate levels of the *same* spin. They found that, at degeneracy, conductance was suppressed due to electron correlation effects. In Ref. [6], the authors realized this system in an InSb nanowire QD. In this QD, they could get a level crossing of same spin thanks to the large Zeeman splittings that were acquired with a magnetic field.

Parity is a property of wavefunctions that can affect the tunneling through the QD and leads. The parity of a wavefunction can be odd or even according to:

$$\psi\left(-r\right) = \pm\psi(r) \begin{cases} even\ parity \\ odd\ parity \end{cases}$$

The tunneling rate of electrons from a state in a lead to a state in the QD is given by the tunneling amplitude t. These amplitudes are given by the overlap of the QD and lead wavefunction. Therefore, the sign of the wavefunction at the overlap affects t. In Ref. [6] they found, both experimentally and theoretically, that the suppression at degeneracy was more extensive if the levels had different parities.

In this work, I investigate if probing the system in Ref. [6] with *thermopower* could give any further insight into the transport mechanisms.

1.2 Thermopower

Heat is often a by-product from conversions of energy, for example in car engines and in power plants. Often this heat is wasted instead of converted into electricity. The usual way to go about, when generating electricity from heat, is to let heat evaporate water and let the steam run a turbine. The mechanical energy from the turbine can then be converted to electricity with a generator. With a thermoelectric material, you can take a shortcut. Utilizing the *Seebeck effect*, where a temperature difference is turned into a voltage, one can directly generate an electric current. If a thermoelectric element in a closed circuit is heated in one end, the temperature difference can drive a current from the heated side to the cooler, or the reversed, and through the circuit. Devices on a nanoscale for thermoelectric applications, reviewed in for example Ref. [7], are expected to greatly improve the performance of thermoelectric materials[8][9].

Thermopower is a measure of the voltage generated by a temperature difference for vanishing current. To get a high efficiency when converting heat to electric current, the thermopower should be high. The focus in this thesis however is not to maximize the thermopower in a quantum dot. There is another aspect to thermopower; it is a way to probe energy features of a system. It can capture properties that conductance can not.

2 Outline

In the theory part of this thesis, I firstly present some basics knowledge of how electrons tunnel through a QD in Sec. 3. In Sec. 4, I go on to describe the model used for transport in this thesis, the second order von Neumann (2vN) approach, which is a generalized master equation approach[10]. This method takes into account features such as Coulomb interaction, interference effects and cotunneling. In the ensuing Sec. 5, I further introduce thermopower; generally and in QDs. I describe the basics of two articles about two QD conductance phenomenons that are important for the work in this thesis. I also describe how the 2vN method is used in the model to calculate the thermopower in a QD.

In the result part, I firstly, in Sec. 6, describe details about the simulated model; a two level QD. In Sec. 7, I present some results from the thermopower simulations and in Sec. 8 a discussion of the results and a quick outlook are presented.

Part II
Theory

3 Quantum dot transport

3.1 Transport in QDs

Fig. 1 shows an example of an arrangement for measuring current through a QD. To allow for transport, the QD is coupled to leads via tunneling barriers. The leads work as electron reservoirs from which electrons can easily be released. The barriers preserve the confinement of the electrons in the QD, but still allow for transport through tunneling. A bias V is applied over the leads and controlled from a power source. The current is measured with an ammeter. In addition, to be able to tune the levels in the dot up and down, a gate voltage V_g is often applied to the QD.
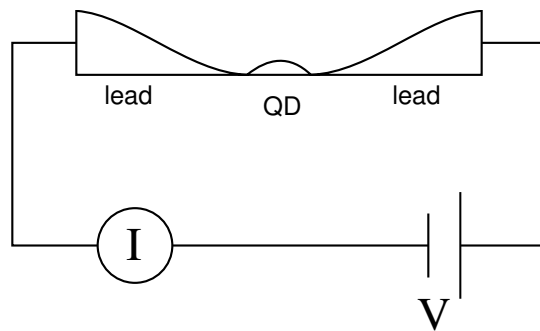

Figure 1: Transport measurement through a quantum dot.

An energy sketch of a QD connected to leads is displayed in Fig. 2a. The chemical potentials, or Fermi levels, of the leads are represented by μ_L and μ_R. I will refer to the energy in between μ_L and μ_R as the Fermi energy E_F. As V will be applied symmetrically around E_F, it will always be in between μ_L and μ_R. In Fig. 2, the QD has four spinless energy levels. Accordingly, there can only be one electron in each level. In an occupied energy level, the electron is represented with a black circle. All energy levels of the QD that are below μ_L and μ_R are occupied while the ones above are empty. This is because an empty level below μ_L and μ_R is instantly filled by the entering of an electron from one of the leads. For a dot level to be occupied, there must be electrons in the leads with the same energy as it takes to enter the level. This is the case below μ_L and μ_R, but not above.
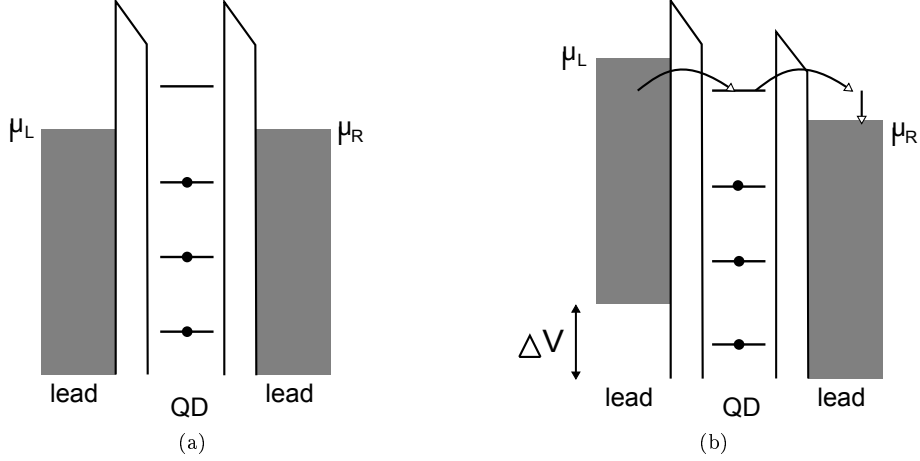
9

Figure 2: A four level QD connected to leads via tunneling barriers. **a)** No current goes through the dot. **b)** With the applied bias over the QD, there can be sequential tunneling. With resonant tunneling, an electron comes into the dot level from the left lead. Again with resonant tunneling, the electron continues to the other lead and relaxes down to the chemical potential.

The largest contribution to the current through a QD comes from *sequential tunneling*. This is the process of one electron tunneling from one lead into the dot and then onwards to the other lead by two uncorrelated resonant tunneling events [1].

In Fig. 2b a bias is applied over the leads. This gives a bias window between μ_L and μ_R. For sequential tunneling to occur, there must be a dot level in the bias window. The potential difference drives electrons from one lead, through the QD, and over to the other in two resonant tunneling events. Once in the other lead, the electron relaxes down to the chemical potential.

3.2   Coulomb blockade

Coulomb repulsion has a large impact on the current through a QD. Because the electrons are confined in such a small volume, the Coulomb repulsion can be on the same energy scale as the level spacing. With Coulomb's law, you find that the interaction between two charges increases with decreasing distance as: $|F| = \frac{1}{4\pi\epsilon_0\epsilon}\frac{|q_1 q_2|}{r^2}$. For a QD with a size of $30nm$, this results in a Coulomb repulsion of $2meV$.

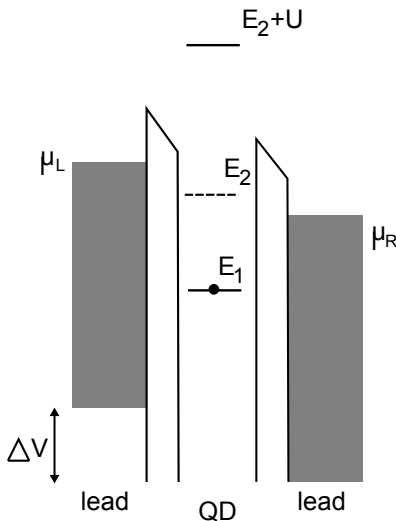In Fig. 3, a two level QD with Coulomb repulsion U is shown.

Figure 3: Coulomb blockade; current through E_2 is blocked because of the Coulomb repulsion from the electron in E_1.

If one level is occupied, it takes U more energy to occupy the other level. In Fig. 3, E_1 is occupied and thus, the energy it takes to occupy the second state is $E_2 + U$. Without interaction, E_2 would be in the bias window and current would flow. To overcome the Coulomb blockade and get sequential tunneling, the gate voltage needs to be tuned so that $E_2 + U$ is in the bias window.

3.3   Second order tunneling

When current is blocked because of Coulomb repulsion, or when there is no level in the bias window, there can not be any sequential tunneling. A smaller amount of current however, can still run through processes of higher order tunneling. The model of transport used in this thesis includes second order tunneling. These are events that include two tunneling events under a short time span. Therefore, if the sequential tunneling rate is Γ, the rate for second order tunneling is Γ^2. Second order tunneling includes *cotunneling* and *pairtunneling*.
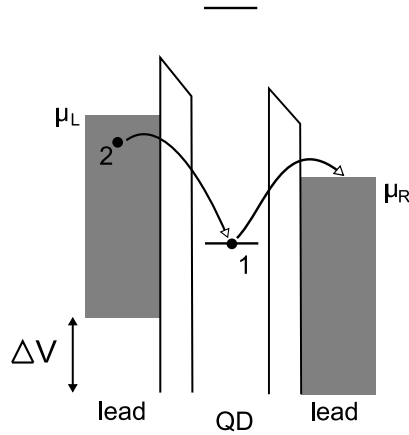
Figure 4: Example of cotunneling: two tunneling events involving two different electrons occur under a short time. The electron labeled 1 tunnels to μ_R after which the electron labeled 2 tunnels into the dot. The dot remains in the same state after the cotunneling, which is called elastic cotunneling.

A cotunneling event is illustrated in Fig. 4. With sequential tunneling, energy is conserved in both tunneling events, in and out of the dot. In Fig. 4, the two separate tunneling events do not conserve energy, but together they do. The two tunnelings can occur if they happen within a short enough time span, as validated by Heisenberg's uncertainty principle, $\triangle E \triangle t \geq \frac{\hbar}{2}$. Cotunneling is either an elastic or inelastic process. The elastic does not affect the total energy of the dot, while the inelastic leaves the dot with a new total energy, i.e., an excited state. To deexcite after an inelastic tunneling event, the QD can either relax with another cotunneling event, with sequential tunneling or with phonon emission. These extra processes result in higher current from inelastic than elastic cotunneling.

Pairtunneling is when two electrons simultaneously tunnel into two different levels in the dot that together conserves energy. These events are normally less common than cotunneling, but for attractive particle interaction, they are dominating the current[11][12].

4 Transport modeling

In this section the second order von Neumann (2vN) approach is introduced. This is the approach used in this thesis for calculating current through a QD connected to leads. This method was first outlined in Ref. [10].

As long as a QD is relatively small, up to around ten electrons, the Eigenstates can be found by solving the Schrödinger equation. In the leads however, there are too many electrons to do this. Here, you are required to make approximations. Using the *density operator* one can describe how the electron density is changing without solving each lead state. The description of the density operator follows the treatment of Ref. [13].

The *generalized master equation approach* is a frequently used method for calculating current through nanosystems. As the name suggests, it is the description of the use of a master equation to calculate the rate of tunneling. A density operator is used to describe the system and the equation of motion for the density operator gives the systems development in time. 2vN is an extension to this approach as it includes additional tunneling effects; cotunneling and coherence. This is done by using a slightly different scheme when solving the equations of motion.

4.1 The density operator

When a system is not in a pure state, but in a statistical ensemble $\{|\psi_n\rangle\}$, it is said to be in a mixed state. Then it is not established what state the system is in, but it has different probabilities to be in any of the states $|\psi_n\rangle$. This should be distinguished from, for example; $|\psi\rangle = \frac{1}{\sqrt{2}}(|a\rangle + |b\rangle)$, where the state $|\psi\rangle$ is in a superposition, i.e., in both states $|a\rangle$ and $|b\rangle$ at the same time.

In contrast to a pure state, a mixed state can not be written as a sum of vectors, as with a wave function. Instead, it can be described by the *density operator* ρ:

$$\rho = \sum_n p_n |\psi_n\rangle \langle\psi_n| \tag{1}$$

where the mixed state is in the state $|\psi_n\rangle$ with probability p_n and the condition $\sum_n p_n = 1$ must be fulfilled. The density operator may be written in matrix form. To do this we choose a basis $\{|i\rangle\}$ and rewrite Eq. (1) by inserting the basis using closure relation:

$$\sum_n p_n |\psi_n\rangle \langle\psi_n| = \sum_{n,i,j} p_n |i\rangle \langle i| |\psi_n\rangle \langle\psi_n| |j\rangle \langle j|$$

The corresponding *density matrix* elements are thus given by

$$\rho_{ij} = \langle i|\rho|j\rangle = \sum_n p_n \langle i|\psi_n\rangle \langle\psi_n|j\rangle$$

The density operator contains all the available information about the mixed state, correspondingly to how the normal wave function describes a pure state. Even for a pure states there can be advantages with the density operator formalism. For a pure state, there is only one possible possibility $p = 1$ and the density operator becomes simply

$$\rho = |\psi_n\rangle \langle \psi_n|$$

The time evolution for the density operator is governed by the von Neumann equation

$$i\hbar \frac{d}{dt}\rho = - [\rho, H] \tag{2}$$

The expectation value for an operator A acting on a mixed state represented by ρ is[14]

$$\langle A \rangle = \sum_n p_n \langle \psi_n \, | \, A \, | \, \psi_n \rangle = \sum_i \langle i|A\rho|i\rangle = Tr\{A\rho\} \tag{3}$$

where "Tr" denotes the *trace* which is the sum of the diagonal elements in a matrix. For a pure state, this becomes simply $\langle A \rangle = Tr\{A\rho\} = \langle \psi \, | \, A \, | \, \psi \rangle$.

4.2 The density operator for composite systems

In this section it will be explained how the density operator formalism can become very useful when applied to composite quantum systems. A composite system consists of two or more subsystems, for example the two subsystems; quantum dot and leads.

Here we consider a composite system consisting of two subsystems S and T. If it is assumed that at some initial time $t = 0$, there is no correlation between the two subsystems, the density matrix for the total system can be factorized as

$$\rho(0) = \rho_S(0) \otimes \rho_T(0)$$

Assume further that at some time t, an interaction starts between the subsystems, for example electron tunneling. If there is correlation between the subsystems the factorization will not hold. There will be mixing between $\rho_S(0)$ and $\rho_T(0)$. An expression for a single subsystem, say S, at any time, is given by the *reduced density operator*:

$$\rho_S = Tr_T\rho \tag{4}$$

s

where Tr_T is the *partial trace* over ρ. The partial trace means that the trace is only over the sub blocks of ρ, belonging to the subsystem T. The reduced density matrix ρ_S contains all the information about the subsystem S that are contained in the total density matrix ρ.

Consider an operator A that only acts on the Hilbert space of S, $\mathcal{H}_\mathcal{S}$. Acting on the total system it is written $A = A_S \otimes I_T$ where I_T is the identity operator of $\mathcal{H}_T$. The expectation value of A (see Eq. (3)) becomes

$$\langle A \rangle = Tr\left\{\rho A_S \otimes I_T\right\} = \sum_{s,t} \langle s| \otimes \langle t| \, \rho A_S \otimes I_T \, |s\rangle \otimes |t\rangle$$
$$= \sum_{s,t} \langle s| \, \langle t| \, \rho \, |t\rangle \, A_S \, |s\rangle = Tr_S\{\rho_S A_s\}$$

So, an observable in subsystem S depends only on ρ_S where the subsystem T is "traced out". The combination of QD and leads constitutes a typical example where this becomes useful. Often one wants to get rid of the part of the density matrix that denotes the leads because they typically have a lot of states.

4.3 Second order von Neumann

In this section the second order von Neumann (2vN) approach is described for a system of a QD connected to two leads. The goal is to find an expression for the current through the system. Thus, we need to know how many electrons that are tunneling from one lead into the dot per unit time. To do this, we need to look at the dynamics of the system via the von Neumann equation and the Hamiltonian involved. This section follows Ref. [15].

4.3.1 The model Hamiltonian

The Hamiltonian considered here has three parts, two describing the subsystems; the QD and the leads, and one describing the tunneling between them:

$$H = H_{QD} + H_{leads} + H_t$$

The details of the respective parts are (written in second quantization formalism):

1. The part governing the quantum dot, without interaction with the leads. It is assumed that H_{QD} is diagonizable, i.e., that the solutions to the Schrödinger equations can be found and thus, the eigenvalues E_a and the eigenstates $|a\rangle$ are known.

$$H_{QD} = \sum_a E_a \, |a\rangle \, \langle a| \tag{5}$$

2. The part governing the leads:

$$H_{leads} = \sum_{k\sigma l} E_{k\sigma l} c_{k\sigma l}^\dagger c_{k\sigma l}$$

where k denotes the lead state, σ spin up or down and l the lead, in this case, the left L or the right R. The lead states are described as free particle states. $c_{k\sigma l}^\dagger / c_{k\sigma l}$ are the creation/annihilation operator which

creates/annihilates an electron in state $k\sigma l$ in the leads. $c_{k\sigma l}^{\dagger}c_{k\sigma l}$ is called the number operator since when it operates on a wave function or a density matrix, it gives back the number of particles in state $k\sigma l$.

3. The tunneling Hamiltonian, describing the tunneling between dot and leads

$$H_t = \sum_{k\sigma l, ab} \left(t_{ba}\left(k\sigma l\right) \left|b\right\rangle \left\langle a\right| c_{k\sigma l} + c_{k\sigma l}^{\dagger} \left|a\right\rangle \left\langle b\right| t_{ba}^{*}\left(k\sigma l\right) \right)$$

where $t_{ba}\left(k\sigma l\right)$ are the *tunneling amplitudes*. These are the probabilities for tunneling from the state $k\sigma l$ in to the dot, thereby changing the dot state from $\left|a\right\rangle$ to $\left|b\right\rangle$. We use the convention that state $\left|b\right\rangle$ contains one more electron than $\left|a\right\rangle$, $\left|c\right\rangle$ one more electron than $\left|b\right\rangle$, and so on.

4.3.2 Second order von Neumann

The QD and the leads constitute the system that 2vN is set out for in this section. The two subsystems, QD and leads, are interacting through electron tunneling. At $t = 0$, if it is assumed that no interaction has started, the density operator can be factorized as $\rho\left(0\right) = \rho_{QD}\left(0\right) \otimes \rho_{leads}\left(0\right)$.

Some formalism is necessary to understand the expression for the current shown below. Both lead states are represented by the state vector $\left|g\right\rangle$. The total system is represented by the tensor product $\left|ag\right\rangle = \left|a\right\rangle \otimes \left|g\right\rangle$. By choosing the basis $\{\left|ag\right\rangle\}$, the matrix elements of the density operator is defined as $\rho_{ag;bg'}^{[n]} = \left\langle ag|\rho|bg'\right\rangle$. The number n in the square bracket $\rho^{[n]}$ denotes the number of electron tunnelings that are involved in bringing the system from state $\left|ag\right\rangle$ to state $\left|bg'\right\rangle$. For example, $\rho_{ag,bg-k\sigma l}^{[1]}$ is the matrix element that denotes the transition between the dot states $\left|a\right\rangle$ and $\left|b\right\rangle$. This transition means that one electron tunnels from one lead into the dot. With that, the lead state changes to $\left|g - k\sigma l\right\rangle$.

The current through the system, J_l, equals the change in population of one of the leads, say the left lead $l = L$:

$$\begin{aligned}
J_L &= -\frac{d}{dt}\sum_{k\sigma L}\left\langle c_{k\sigma l}^{\dagger}c_{k\sigma l}\right\rangle = -\frac{d}{dt}\sum_{k\sigma L, bg}\rho_{bg,bgk\sigma l}^{[0]} \\
&= -\frac{2}{\hbar}\sum_{k\sigma L, cb}Im\left(\sum_{g}t_{cb}^{*}\left(k\right)\rho_{cg-k\sigma l, bg}^{[1]}\right)
\end{aligned} \tag{6}$$

The average of the number operator, $\left\langle c_{k}^{\dagger}c_{k}\right\rangle$, for all values of $k\sigma L$ gives the population. After the second equality sign, with use of Eq. (3), this is instead expressed in terms of the density matrix. In the density matrix, it is the diagonal elements, $\rho_{bg,bgk\sigma l}^{[0]}$, that represent the populations.

With the sum $\sum_{g}$ in Eq. (6), summing over all the lead states, the advantage with density matrix formalism appears. When all lead states are summed over, the resulting density matrix becomes a much smaller, more manageable matrix with the dimensions of the number of states in the dot.

To study how the current changes in time we need to study the equation of motion for the matrix elements in Eq. (6). The sum $\sum_g$ is first performed, then the matrix elements are inserted into the von Neumann equation, Eq. (2). The resulting equation is a differential equation where the time dependence of the $\rho^{[1]}$ elements depends on $\rho^{[0]}$ and $\rho^{[2]}$ elements. Thus, the equation of motions for these $\rho^{[0]}$ and $\rho^{[2]}$ elements needs to be studied as well. As it turns out, all matrix elements $\rho^{[n]}$ depend on higher orders of n. This results in an infinite set of differential equations. To get a solution, it is necessary to make approximations. In 2vN, all matrix elements $n \geq 3$ are put to zero. Beyond that, a few further approximations need to be performed before the system of equations can be solved, see Ref. [15].

4.3.3   Review

There are different ways to make the approximations and truncation that are necessary in order to solve the equation of motion for the density matrix.

$\sum_g \rho^{[0]}$ is the reduced dot density matrix ρ_{dot}, see Eq. (4). In the master equation approach, the current is approximated to depend only on the populations; the diagonal elements of ρ_{dot} . In this case, the current is composed of sequential tunneling events that are incorporated in ρ_{dot} via H_t .

In the *generalized* master equation approach, the off-diagonal matrix elements of ρ_{dot} are also included. These matrix elements correspond to coherence, or, superpositions between dot states. With that, the possibility is included, that when an electron passes through the system, it goes through two dot levels at the same time.

The 2vN approach goes beyond that, as elements $\rho^{[2]}$ from the total density matrix are also included. These elements correspond to second order tunneling. As the $\rho^{[0]}$ and $\rho^{[1]}$ elements depend on $\rho^{[n]}$ for higher values of n, these elements become more exact with the inclusion of $\rho^{[2]}$ elements.

The choices of approximations and truncation level should depend on the systems properties such as; energy configuration and coupling strength. The properties settle which quantum effects and components to the current that are essential to the accuracy. In 2vN, all $n \geq 3$ is put to zero. This approximation works for the coupling strength between leads and dot that is used in this thesis. For stronger coupling strength, higher order tunneling might become important. A topic that is discussed in this thesis is Coulomb blockade, described under section 3.2, where single electron tunneling is blocked. Under these conditions, second order tunneling becomes crucial as it is the first non-vanishing order.

5 Thermopower

5.1 Thermopower

Consider a rod of an arbitrary material, isolated from its surroundings, with different temperatures at its two ends. As an isolated system always goes towards thermal equilibrium, as time goes, the temperature difference in the rod will start to even out. Heat in materials is transported in two ways; by lattice vibrations (phonons) or charge carriers, i.e., mainly electrons or holes. The thermal conductance, the ability to transport heat, is denoted by $\kappa = \kappa_e + \kappa_{ph}$.

The density of free carriers throughout the rod will be the same, however, the ones in the hot end will have higher momenta. Thus, there will be a net diffusion of charge from the hot to the cold end. The drifting charge carriers give rise to an electrical current I as well as a heat flow J. The electric current is defined by the flow of electric charge per second ($\frac{C}{s}$), while the heat current is the amount of heat carried by the charge carriers per second ($\frac{J}{s}$). With more charge carriers ending up at the cold end than the hot, there will be a voltage drop over the rod. The build up of a voltage due to a temperature difference is called the *Seebeck effect*. This is parametrized by the *Seebeck coefficient*, or, *Thermopower*. Thermopower is defined by this voltage V when the current I is zero, divided by the temperature difference:

$$S = -\left.\frac{V}{\Delta T}\right|_{I=0} \tag{7}$$

This definition holds for small temperature differences, thus near equilibrium. The sign of the voltage will be opposite if the majority of charge carriers are electrons or holes. With this definition, the thermopower will be negative when the current is carried by electrons and positive for holes. If there are an equal amount of both, drifting to the colder end, their charge will cancel and there will be no voltage build up. This is why metals, with half filled bands and thus similar amount of free electrons and hole charge carriers, have small thermopowers[16]. Semiconductors can be doped to have only one sort of free charge carrier and thus acquire large thermopowers[16].

The 'figure of merit' is a quantity used to give a notion of the performance of a device relative to others. For the ability to convert heat to electrical current the figure of merit ZT is defined as [17]

$$ZT = \frac{S^2 \sigma T}{\kappa} \tag{8}$$

For a good conversion, the thermopower S should be high, i.e., a large voltage response to a given temperature difference ΔT. The electric conductance σ ($\frac{C}{Vs}$) describes how easily the charge carriers travels from the hot to cold end. Together $S^2\sigma$ is proportional to the power production of the device[18]. The thermal conductance κ ($\frac{J}{s^2}$) is in the denominator as it stands for the ability to conduct heat and thus remove the temperature difference. For a high ZT,

the temperature difference should be easy to maintain. For a useful device, ZT should be equal to one or higher.

The thermal and electrical conductances are closely related through the Wiedemann-Franz law:

$$\kappa = \sigma l_0 T$$

where $l_0 = \frac{\pi^2}{3}\frac{k_B^2}{e^2}$ is the Lorentz number. This brings on a conflict in the ZT expression as you want the electric conductance to be high but the thermal conductance to be low. A high ZT can be acquired in devices for which the Wiedemann-Franz law breaks down, which can be the case in nanosystems[19].

5.2 Thermopower in a QD

In the rod from the last section, the charge carriers give rise to a voltage because the hot carriers are more mobile, they have higher energy, than the cold ones and diffuse easier. In a system of a QD connected to leads, the transport mechanism is not diffusion but tunneling. Tunneling through a QD is energy dependent because of the QD's discrete energy levels, but a higher energy does not equal higher tunneling probability than a lower energy. Even so, a temperature difference over a QD can create a thermocurrent.

In this section, thermopower will be discussed for the system used in the simulations of this work. The system is outlined in Fig. 5, with a Coulomb repulsion that is smaller than the QD's levels spacing. In this work, the QD coupled to leads are modeled as an *open system* which means that the temperatures of the leads will be constant. A temperature difference between the leads will lead to a current if there are suitable QD levels, but it will not give rise to a voltage between the leads. The thermopower is then defined as the applied voltage it would take to counteract the flow of electrons induced by the temperature difference. The voltage is given by

$$V = \frac{\mu_L - \mu_R}{-e}$$

In this work, metallic leads are considered, thereby the occupation of carriers follows the Fermi function:

$$f(E) = \frac{1}{1 + exp\left(\frac{E-\mu}{k_B T}\right)}$$

Consider a temperature difference between the leads $\Delta T = T_{hot} - T_{cold}$. The Fermi function of the warmer lead has got a larger spread around its chemical potential, see Fig. 5. At energies above the Fermi level, there are more electrons in the hot lead than in the cold. At the same time, there are more electrons in the cold lead at energies just below the Fermi level. At the Fermi level, there are equal amount of electrons in both. Given that there are available energy levels that can conduct the current, the difference in occupations gives electric currents. A larger difference will give a larger current.
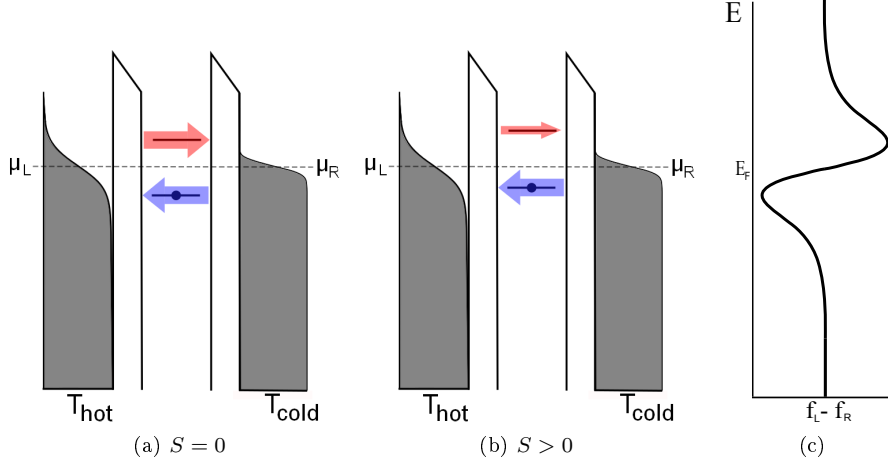
Figure 5: A two level QD connected to leads of different temperatures $T_{hot} > T_{cold}$. The Fermi distributions of the leads are outlined. **a)** The levels are situated symmetrically around the chemical potential. For equal coupling strength, the current that goes through the upper and lower level will be equal and the net current zero. **b)** The lower level is closer to the chemical potential than the higher. Therefore, more current will run through the lower level. The net current is non-zero and consequently the thermopower is non-zero. **c)** A sketch of $f_L - f_R$.

In Fig. 5a, a current runs from the hot to the cold lead through the QD level situated above the Fermi level. Another current runs in the opposite direction via the level below the Fermi level. Provided that the levels have equal coupling strength and are at the same distance from the Fermi level, both currents will be of equal size and the net current becomes zero. The transport in the filled levels below the Fermi level is in solid state physics formalism said to be carried by a hole. At this configuration, electrons and holes here contribute equally to the current. This will be referred to as the *electron hole symmetry point*.

If the current is zero for $V = 0$, the thermopower, Eq. (7), is zero. Energy is still transferred from the hot to the cold lead with a heat current. The amount of charge carriers tunneling to the right and left may be equal, but the electrons tunneling from the hot to the cold lead have higher energy and are thus carrying more heat.

Whenever the temperature difference of the leads creates a net thermocurrent, the thermopower will be non-zero. In Fig. 5b the lower energy level is situated closer to the Fermi level than the one above. Presuming equal coupling strengths, the current via the level that is closer to a maximum of $f_L - f_R$ will be larger. Therefore, there will be a net thermoelectric current going below E_F. In other words, the largest part of the current is carried by holes. This can be read from the sign of the thermopower, which is positive.

5.3 Single level QD thermopower lineshape using transmission formalism

In this section follows a short description of the thermopower lineshape of a single level QD, that is, how the thermopower depend on the chemical potential. In Ref. [20], it is concluded that the lineshape of a QD depends on the parameters $k_B T$, Γ and ΔE's relative magnitude.

Without considering any interactions, the thermopower can be calculated using transmission formalism. For non interacting electrons, the current through the QD can be calculated with the *Landauer-Büttiker formula*:

$$I = \frac{-2e}{h} \int\limits_{-\infty}^{\infty} (f_L(E) - f_R(E)) T(E) dE \qquad (9)$$

The transmission function $T(E)$ can be approximated with *the Breit-Wigner formula*. For one energy level it reads

$$T(E) = \left| \frac{\Gamma}{E - E_1 + i\Gamma} \right|^2 \qquad (10)$$

In Fig. 6 is an example of the thermopower S in a single level QD coupled to leads of different temperatures, as a function of the energy of the eigenstate E_1. The current is calculated with the Landauer-Büttiker formula, Eq. (9) and S is found with Eq. (7).
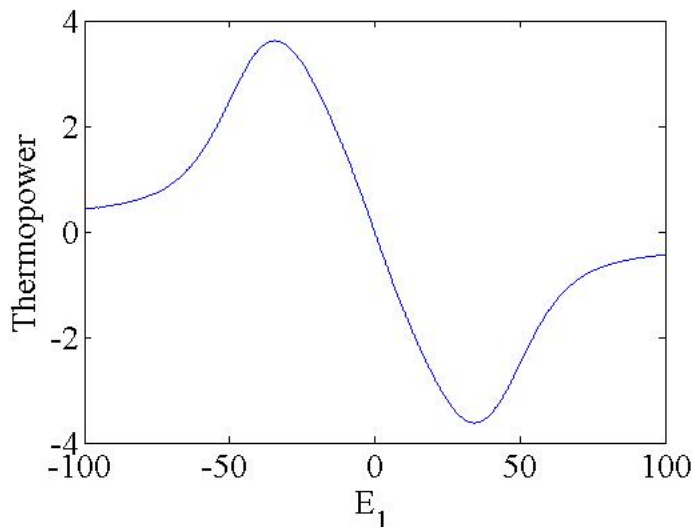

Figure 6: Thermopower as a function of E_1 in a single level QD. Parameters used are: $E_1 = V_g$, $k_B T_L = 6.05$, $k_B T_R = 6.00$ and $\Gamma = 1$ using arbitrary units. The energy scale in transport through nanosystems is $\Gamma \sim 0.1 meV$.

From Eq. (9), it appears that $I = 0$ if either of the terms $f_L(E) - f_R(E)$ or $T(E)$ equals zero. In Fig. 6, when E_1 is at the Fermi energy $E_F = 0$, then $f_L(E_1) - f_R(E_1) = 0$ and $I = 0$. From the definition of thermopower, Eq. (7), it is evident that $S = 0$ at this point because the voltage it takes to get zero current is $V = 0$. The function $T(E)$ in Eq. (10) is centered around E_1, so when E_1 is at an energy where $f_L(E) - f_R(E) \neq 0$, a bias $V \neq 0$ is required to get $I = 0$.

Initially, $|S|$ grows as E_1 is tuned away from E_F. This is because then, the largest contribution to the current comes from electrons tunneling at energies around E_1, where $T(E)$ is at its maximum. Accordingly, to get $I = 0$, V is increased. However, as E_1 is tuned away from E_F, the contribution from electrons tunneling in the tail of $T(E)$, around E_F, increases. When $|S|$ starts to decrease at around $E_1 = \pm 34$, the contribution to I due to tunneling in the tail exceeds tunneling around the $T(E)$ maximum. Then tunneling again occurs close to E_F and a smaller V is required for $I = 0$. If the transmission function was a delta function, S would just keep growing linearly with E_1. But, as S reaches its maximum, the finite width of $T(E)$ means that electrons can tunnel away from the energy E_1.

From the sign of S, one can conclude whether the largest part of the current is carried by electrons or holes. When E_1 is below E_F, the average tunneling charge carrier is a hole and thus, S is positive. When E_1 is over E_F, there are mostly electrons contributing to the current and S is negative.

It is evident that S gives information about the energies where tunneling occurs. According to Ref. [21], thermopower is in fact "a measure of the average energy that the electrons carry during tunneling processes".

The transmission formalism does not distinguish between different kinds of tunneling. However, in Ref. [21] it is outlined that the linear increase in S is due to sequential tunneling, while after S reaches its maximum, second order tunneling takes over. The electrons involved in second order tunneling pertains to energies around the Fermi level; that is why there is a sudden decrease in S when those processes become more probable.

5.4   Optimizing the transmission function

For simplicity, the energy levels in the sketches presented so far have been drawn as plane lines. The lines do however, posses a linewidth that depends on their coupling strength. Looking at Eq. (8), it is evident that, to get a good heat to current performance, the thermopower should be high. To acquire a QD with a high thermopower, the configuration should enable a large current in one direction. In Ref. [22], the author found that the optimal transmission function for maximum thermoelectric efficiency is one that enables tunneling in a certain energy span, but none outside, i.e., one that behaves like a *boxcar function*. (This is suggested to be implemented by putting several QDs in a row, producing a total transmission function in a boxcar form.) The natural linewidth of QD energy levels, however, is not similar to a boxshape.

To get a large current through a single level with a Lorentzian shape, the

broadening of the level should be sufficiently large to enable tunneling at many energies, i.e., a broad transmission function. Furthermore, the transmission function should be centered sufficiently close to the chemical potential where the difference between the Fermi distribution functions is the highest, i.e., the tunneling rate is the highest. These two arguments together give a poor performance due to the effect illustrated in Fig. 7. When the broadening of a level is wide enough to spread over the Fermi level, this enables tunneling in the other direction. If the center of the transmission function is at the Fermi level, then two equal currents would go in the right and left direction. If the center is just above the Fermi level, the largest current would go to the right but still a large current would go to the left. To maximize the thermopower, a balance between the width and position of the level needs to be found.
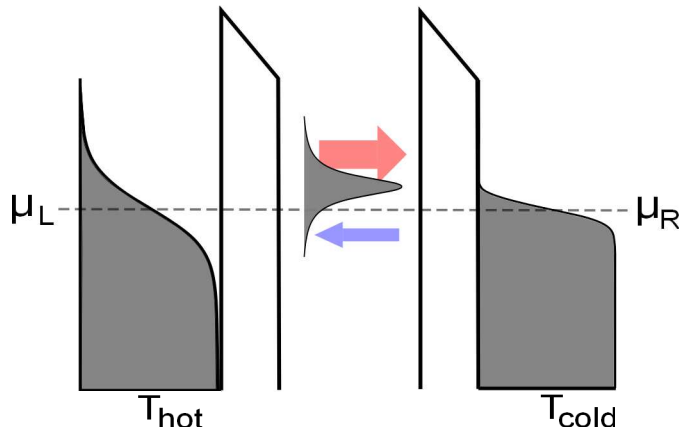

Figure 7: Transmission function for a single level QD. The tail of the transmission function goes over the chemical potential of the leads. This enables tunneling in the left direction as well as in the right direction.

In Ref. [23], the authors have made a trick to overcome the problem with counteracting currents. The goal was to increase the net current by getting rid of the current running in the left direction in Fig. 7. The authors have come up with a quantum system which achieves a transmission function that essentially only gives current in one direction. The main things about this system is that it is a two level system where the two levels have different parity. The tunneling amplitudes are chosen as: $t_{L1} = t$ $t_{R1} = t$ $t_{L2} = -at$ $t_{R2} = at$ where a is a real constant. The parity difference manifests itself in that sign difference between the tunneling amplitudes. The tunneling amplitudes are given by the overlap of the QD and lead wave functions. The eigenfunction to E_1 should have even parity, then the function will have the same sign at the overlap to the left lead as to the right lead. The eigenfunction to E_2 should have odd parity, to achieve different signs of the function at the overlap to the left lead and the right lead. The specified tunneling amplitudes result in the following coupling strengths:

$\Gamma_{L1} = \Gamma_{R1} = \Gamma$ and $\Gamma_{L2} = \Gamma_{R2} = a^2\Gamma$. Furthermore, the energy levels, E_1 and E_2, should always be situated on the same side of E_F. If both levels are above the Fermi level, that means that no level is occupied and then Coulomb repulsion will not play any role for transport. Therefore, transmission function formalisms, as discussed in Sec. 5.3, can be used. For a system with two energy levels, E_1 and E_2, the Breit-Wigner formula reads:

$$T(E) = \Gamma^2 \left| \frac{1}{E - E_1 + i\Gamma} - \frac{a^2}{E - E_2 + ia^2\Gamma} \right|^2 \tag{11}$$

The minus sign between the two terms in Eq. (11) comes from the sign difference of the tunneling amplitudes. This means that there is destructive interference between the two levels. Interference between energy levels can be used to 'taylor' the transmission function. If $E_2 = a^2 E_1$, then $T(0) = 0$ at the Fermi energy $E_F = 0$, so with that level configuration there will be no transport at the Fermi energy. Furthermore, depending on which side E_1 and E_2 are of E_F, the transmission function will be lower on the opposite side of E_F. By optimizing the *power factor*, $S^2\sigma$, by means of changing a, Γ, E_1 and E_2, the authors obtained the transmission function in Fig. 8. The transmission function is cut off at E_F resulting in that almost all current will go in one direction, giving a high thermopower.
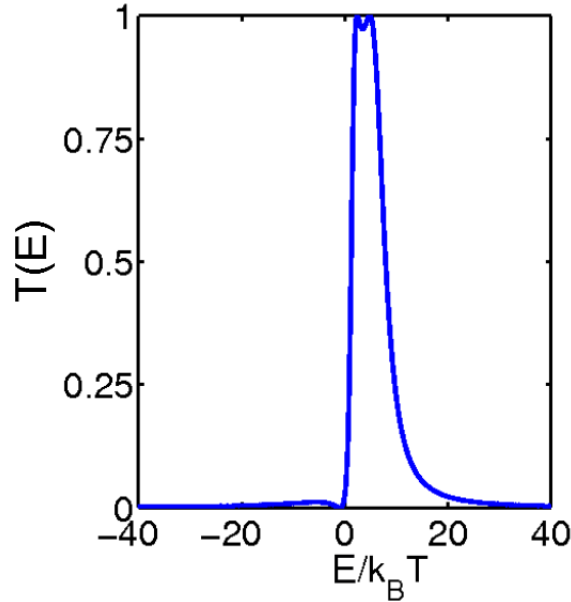

Figure 8: Figure taken from Ref. [23] Figure 3. Transmission function of two level QD optimized for high power factor.

5.5 Canyon of current suppression

When electrons tunnels through a QD with more than one energy level there can be interference. The simplest system to investigate this is a two level spinless system, that is, with both levels having equal spin and accordingly only one electron at a time can occupy each level. In Ref. [6], the authors give an account for the findings of a non intuitive conductance plot of such a system coupled to two leads. What is expected is high conductance when the configuration allows for sequential tunneling, and lower conductance in the Coulomb blockade region. However, in Ref. [5], the authors found a suppression of conductance in the Coulomb blockade region in this system. Furthermore, in Ref. [6], it is found that the conductance is suppressed at level degeneracy both in the Coulomb blockade region *and* in the sequential tunneling region. They refer to this phenomenon as *the canyon of current suppression* which is further investigated in Ref. [24].

In Ref. [6], a two level spinless system was realized in a InSb nanowire QD. Thanks to large g-factors, they were able to get two degenerate levels of the same spin at the single particle states 4 and 5 by applying a magnetic field, as depicted in Fig. 9 at point 'S'. At this configuration, the QD is a spinless system, that is, both levels have equal spin and accordingly only one electron at a time can occupy each level.
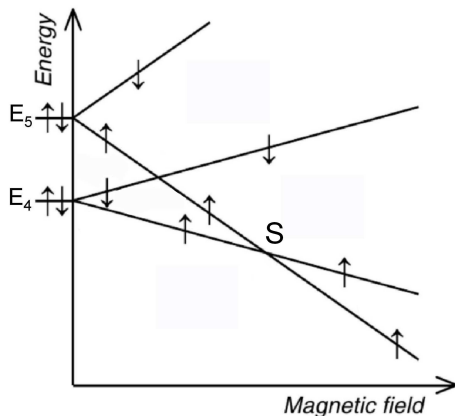

Figure 9: Figure taken from Ref. [6] Figure 1c. Schematic illustration of the evolution of two single particle energy levels in a magnetic field. Coulomb interaction is neglected. At point S, there is a level crossing of two energy levels with the same spin.

What is causing the suppression of current is a parity difference between the two energy levels. If the parity of the QD state is odd, the sign of the wavefunction will be different at the overlap to the left lead than to the right lead. If the parity is even, it will have the same sign. Therefore, if the parity of a QD state is odd, t_L and t_R will have different signs. If state E_1 is even and

state E_2 is odd, the tunneling amplitudes are: $t_{L1} = t$, $t_{R1} = t$, $t_{L2} = -at$ and $t_{R2} = at$ where a is a real constant.

The conductance G is defined as

$$G = \frac{I}{V}\bigg|_{\Delta T = 0} \tag{12}$$

A simulation of the system in Ref. [6] is shown in Fig. 10. Here G is plotted as a function of gate voltage V_g and magnetic field B and the canyon of current suppression is present.
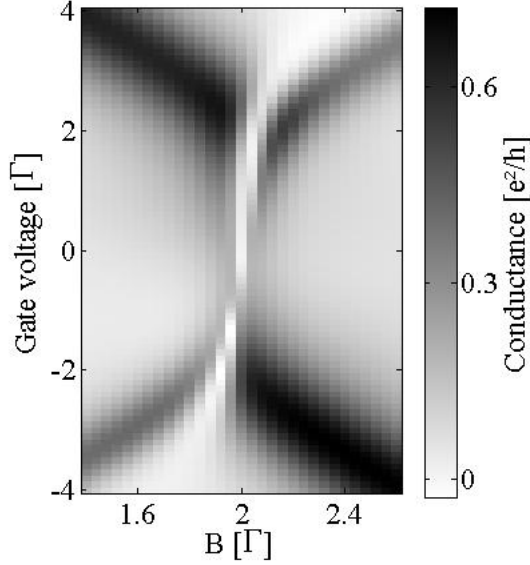

Figure 10: Conduction plot showing the canyon of current suppression. The parameters used are $k_B T = 0.2\Gamma$, $U = 5\Gamma$, $t_{1L} = -\sqrt{0.3}$, $t_{1R} = \sqrt{0.1}$, $t_{2R} = \sqrt{0.4}$, $t_{2L} = 1$ and $V_{bias} = 0.5\Gamma$. The energy levels are given by $E_1 = -6.5 - V_g + 2B$ and $E_2 = 2.5 - V_g - 2.5B$ and are thus degenerate at $B = 2\Gamma$.

The black lines of high conductance is due to sequential tunneling, arising when an energy level is in the bias window. The line starting at the top left corner is at the configuration when E_1 is occupied and $E_2 + U$ is in the bias window. This line is cut off at around $B = 2\Gamma$ when the energy levels are degenerate. The interrupted line continues up to the top right corner where instead E_2 is occupied and $E_1 + U$ is in the bias window. There is higher conductance when $E_2 + U$ is in the bias window since E_2 has higher coupling strength. In the same manner, the high conductance lines in the bottom of the figure emerge when either E_1 or E_2 is in the bias window.

Outside the Coulomb blockade region, the current can be approximated by neglecting Coulomb interaction. Here, transmission function formalism can be

used, see Eq. (9) and Eq. (11). The sign difference between the tunneling amplitudes results in a minus sign between the two terms, representing each QD state, in Eq. (11). With the level configuration $E_2 = a^2 E_1$, the two terms totally cancel and $T(0) = 0$. That is why the sequential tunneling lines in Fig. 10 are suppressed close to degeneracy, $B \approx 2$, where the energy levels experience a lot of destructive interference.

The area in between these lines is the Coulomb blockade region. The canyon of current suppression, that cuts off the sequential tunneling lines, continues also throughout this region. Here, the current is carried by higher order tunneling. The electron hole symmetry point is at $V_g = 0$. At this point, second order tunneling currents completely cancels and there is a complete suppression of the current. The complete suppression will hold in the limit of zero bias and $k_B T$, when it is only electrons close to the Fermi energy that are involved in tunneling. These electrons require equal amount of energy to tunnel via E_1/E_2 and $E_1 + U/E_2 + U$. In the other parts of the Coulomb blockade region, the current is not zero but only partly suppressed.

5.6 Thermopower with 2vN

The code simulating the thermopower in this thesis is constructed as follows. A temperature difference between the two leads $\Delta T = T_L - T_R$ is set. The chemical potentials is initially set to $\mu_L = \mu_R = 0$. The current I is calculated using the 2vN approach described in Sec. 4. The temperature difference ΔT will generate a current $I \neq 0$. To obtain the thermopower, the voltage at which the current becomes zero needs to be found. This is done with an iterative procedure. A voltage is applied so that a current runs in the opposite direction to the thermoelectrically induced current. The voltage is applied symmetrically, i.e., $\mu_L = x$ and $\mu_R = -\mu_L$. After a first guess of x, the current is evaluated with the 2vN program. After that, x is changed with a smaller and smaller step size, the closer I is to zero. When the voltage difference is such that the net current becomes zero, the thermopower can be acquired by dividing the voltage with the temperature difference, see Eq. (7).
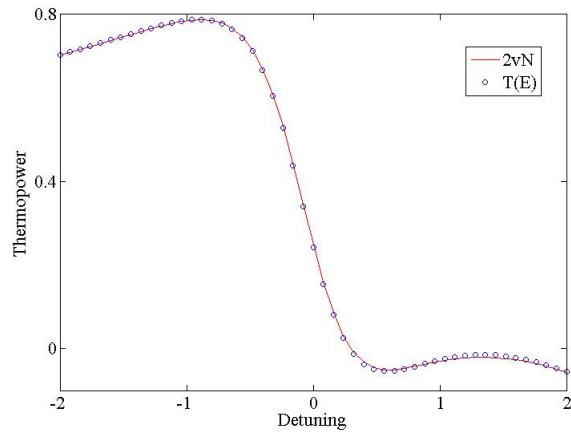
Figure 11: Thermopower S as a function of level detuning calculated with second order von Neumann method (2vN) and with transmission function, $T(E)$, approach. The parameters used are $\Gamma = 1$ and $a = 0.5$, $k_B T = 1.00\Gamma$ and $\triangle k_B T = 0.10\Gamma$, with $E_1 = -0.5 + \frac{\Delta E}{2}$ $E_2 = -0.5 - \frac{\Delta E}{2}$. Arbitrary units are used.

Thermopower for a two level QD without Coulomb interaction, calculated with the Landauer-Büttiker formula, Eq. (11), and the 2vN method is shown in Fig. 11 for benchmarking purposes.

28

Part III
Results

6 The model

The system under investigation in this project is a two level spinless quantum dot coupled to two leads. The energy levels of the dot in the Hamiltonian, Eq. (5), are modeled as

$$E_1 = E_{01} - V_g + g_1 B$$

$$E_2 = E_{02} - V_g + g_2 B$$

where a gate voltage V_g steers the dot's energy levels position while a magnetic field B controls the level detuning, i.e., $E_1 - E_2$. The bias over the QD is applied symmetrically over the Fermi level so that $\mu_L = V/2$ and $\mu_R = -V/2$. The coupling strengths are given by $\Gamma = 2\pi t^2 \rho_0$, where the density of states ρ_0 is chosen to be constant, $\rho_0 = \sum_k \delta(E_k - E)$.

7 Results

7.1 Overview

In Sec. 7.2, I show the conductance G and thermopower S from simulations of a two level spinless QD. The two levels have equal coupling strengths but different parities. This leads to a canyon of full current suppression, as described in Sec. 5.5.

In the subsequent Sec. 7.3, I turn to the case of different coupling strengths, again simulating conductance and thermopower. While equal coupling strengths make it straight forward to predict the effect of varying the Coulomb repulsion U, different coupling strengths complicate it. When this was studied, an interesting change was found in the thermopower simulations when U was varied.

In Sec. 7.4, I investigate if the pattern in Sec. 7.3 can be repeated for another set of parameters. The parameters chosen for this purpose were taken to reproduce the canyon of current suppression that is experimentally verified in Ref. [6].

The thermopower in the parameter space of the canyon of current suppression was investigated. I wanted to find out how the thermopower simulations would compare to the conductance simulations. All simulations were carried out with the 2vN method. The reason I plotted the square root of the absolute value of the thermopower in the following plots is to make sign shifts clearly visible.

7.2 Symmetric coupling strengths

One goal of this project was to investigate the thermopower for the QD described in Ref. [6]. To start off, a similar but simpler simulation was run, where the coupling strength of both levels was put to equal. This was done to get a result that would be easier to interpret. In this simulation, the tunneling amplitudes t are the same for both levels on both sides except for a minus sign. The minus sign is a detail that is crucial, as it brings about the canyon of current suppression. This simulation is seen in Fig. 12 where the square root of the absolute values of thermopower is plotted along with the corresponding conductance plot.
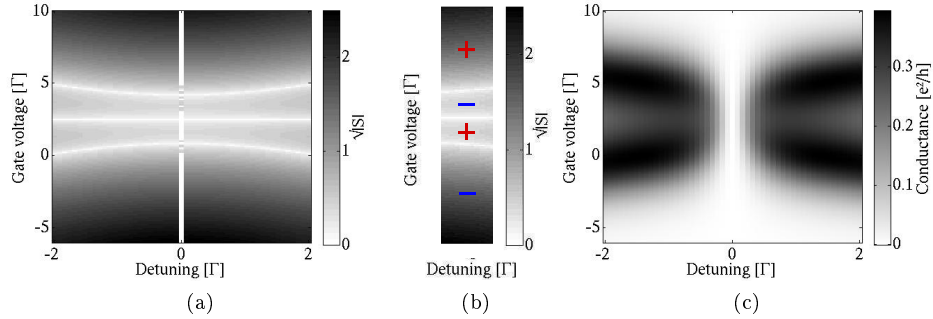

(a) (b) (c)

Figure 12: Simulation of a two level QD. The tunneling amplitudes were $t_{1L} = t_{1R} = t_{2R} = 0.7$, $t_{2L} = -0.7$, $E_{01/02} = 0$, $g_{1/2} = \pm 1$ and the Coulomb repulsion was $U = 5\Gamma$. **a)** The square root of the absolute value of thermopower at a temperature difference between the leads of $\triangle k_B T = 0.10\Gamma$ and $k_B T = 1\Gamma$. **b)** A cut of the thermopower with signs to clarify where S is positive and negative. **c)** Conductance at a bias $V = 0.5\Gamma$ and $k_B T = 1\Gamma$.

The regions with highest conductance in Fig. 12c are sequential tunneling lines and in between them is the Coulomb blockade region. Both regions are cut off around zero detuning, where $E_1 = a^2 E_2$ since $a = 1$, by a canyon of current suppression.

Both figures are full of symmetry. The thermopower plot in Fig. 12a is symmetric around the middle horizontal line at $V_g = 2.5\Gamma$ where $S = 0$. Here the gate voltage is exactly half of the Coulomb repulsion $U = 5\Gamma$. Therefore the singly and doubly occupied states are symmetrically placed around the Fermi level $E_F = 0\Gamma$.

Sequential tunneling can occur for electrons in the leads which resonate with an energy level. As there are more electrons at energy $E = 2.5\Gamma$ in the hot lead than in the cold, there is a current from the hot to the cold lead. In the same way, there is an overflow of electrons in the cold lead at $E = -2.5\Gamma$, leading to a current in the opposite direction. The tunneling amplitudes are of equal size, so these currents are of equal size and cancel each other out so that there is no resulting current. Contributions from second order tunneling also cancel out at

the electron hole symmetry point.

There is another zero thermopower line, extending vertically at zero detuning. At zero detuning the energy levels are degenerate. At degeneracy, the parity difference between the levels means that no current will flow through the QD, as can be seen in the conductance plot Fig. 12c. Coherence effects entails that there can be no first or second order tunneling, as explained in Sec. 5.5. Thermopower is a measure of the average energy of tunneling electrons. If there can not be any transport then the thermopower is undefined. The line does not indicate that the thermopower goes down to zero and there is no sign shift between left and right half of the plot. In contrast, in the three horizontal lines, the thermopower goes down to zero and the sign of the thermopower is altered. When S is negative, most electrons tunnel from the hot to the cold lead. For positive S, most electrons tunnel from the cold to the hot lead. In other words, electrons dominate the tunneling for negative S while holes dominate for positive.

Both remaining zero thermopower lines, placed symmetrically over and below the line at $V_g = 2.5\Gamma$ arise at the same configurations as the sequential tunneling lines in the conductance plot, Fig. 12c. While the conductance reaches maximum at these points, the thermopower experiences a sign shift. This is because, when there is a level crossing, there will be equal amount of tunneling going in both directions, and so the average energy of the tunneling electrons will be zero.

The distance between the outer lines is approximately the magnitude of the Coulomb repulsion U. That distance would grow for increasing U and shrink for decreasing U.

7.3 Asymmetric coupling strengths

Much of the symmetry in the simulations is lost when changing the asymmetry parameter from $a = 1$ to $a = 0.5$. I start to investigate this case for $U = 10\Gamma$, see Fig. 13.
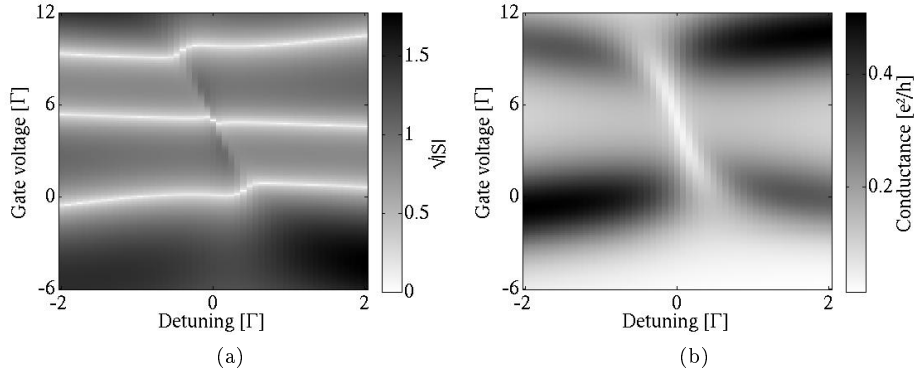
Figure 13: The parameters used were $U = 10\Gamma$, $t_{1L} = t_{1R} = 1$, $t_{2R} = 0.5$, $t_{2L} = -0.5$, $E_{01/02} = 0$ and $g_{1/2} = \pm 1$. **a)** The square root of the absolute value of thermopower at $\triangle k_B T = 0.10\Gamma$ and $k_B T = 1.00\Gamma$. Thermopower shifts sign three times; at the white zero-lines. **b)** Conductance at $V = 0.5\Gamma$ and $k_B T = 1.05\Gamma$.

In the conductance simulation in Fig. 13b, we now see a tilted canyon in contrast to the straight one in Fig. 12c. Another distinction is that the current suppression is not complete away from electron hole symmetry. Furthermore, the sequential tunneling lines have different conductance for positive and negative detuning. These changes arise due to the switch to different coupling strengths. The conductance in the sequential tunneling areas is higher at the detuning where the stronger coupled level crosses the Fermi level.

In the preceding simulation, Fig. 12, with equal coupling strengths, i.e., $a = 1$, the sequential tunneling areas are suppressed at level degeneracy where $E_2 = a^2 E_1$. The condition that $E_2 = a^2 E_1$ to get $T(E) = 0$, I interpret as that the energy states should be, not degenerate, but evenly populated to get zero transmission. In Fig. 12, both levels have a fifty percent chance of being populated at level degeneracy. In Fig. 13b, at $V_g \approx 0$ and level degeneracy, the fact that $\Gamma_1 > \Gamma_2$, means that E_1 has a broadening that reaches further down to lower energies and with that, have a larger probability to be populated. The levels are more evenly populated at a small positive detuning where the weaker coupled level E_2 is lower in energy. Thereby, the sequential tunneling area is suppressed, although not fully, at a small positive detuning. At the sequential tunneling suppression at $V_g \approx 10$, the weaker coupled level is lower for negative detuning. Hence, we end up with a tilted canyon.

Turning to the changes in thermopower, one can see that the undefined line at zero detuning found in Fig. 12a is not present in Fig. 13a. Because of the difference in coupling strengths, the more strongly coupled level can contribute more to transport then the other and current is no longer blocked at level degeneracy. The configurations at which one will find the canyon in the conductance also manifests itself in the thermopower figure. One can see that

the thermopower is changing faster in that area.

The three horizontal zero thermopower lines in Fig. 12a are again found here in Fig. 13a. Again, the middle horizontal line indicating electron hole symmetry and the others an energy level crossing the Fermi level. Because of the difference in coupling strengths, the three zero thermopower lines have bumps around zero detuning. Which levels are carrying the current alternates for positive and negative detuning, therefore there is a bump when they are tied together.

The lower zero thermopower line indicates the level crossing of the singly occupied QD while the upper the doubly occupied. By lowering U, the upper and middle line should come closer to the lower. This is evident from Fig. 14a where $U = 7\Gamma$.

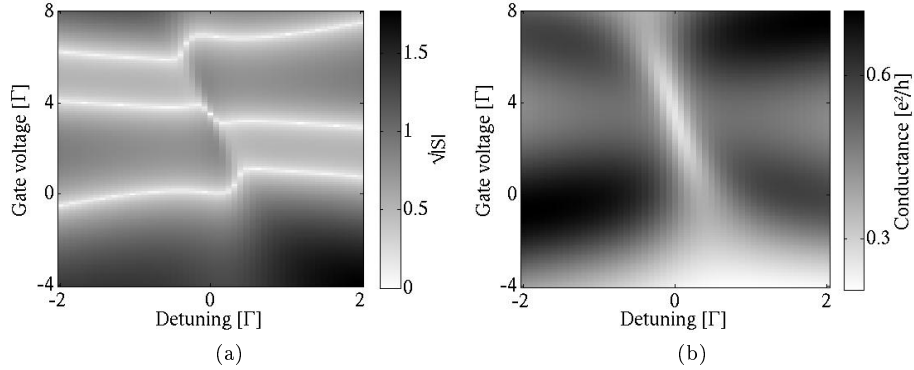(a)   (b)

Figure 14: The parameters used were $U = 7\Gamma$, $t_{1L} = t_{1R} = 1$, $t_{2R} = 0.5$, $t_{2L} = -0.5$, $E_{01/02} = 0$ and $g_{1/2} = \pm 1$. **a)** The square root of the absolute value of thermopower at $k_B T = 1.00\Gamma$ and $\triangle k_B T = 0.10\Gamma$. **b)** Conductance at $V = 0.5\Gamma$ and $k_B T = 1.05\Gamma$.
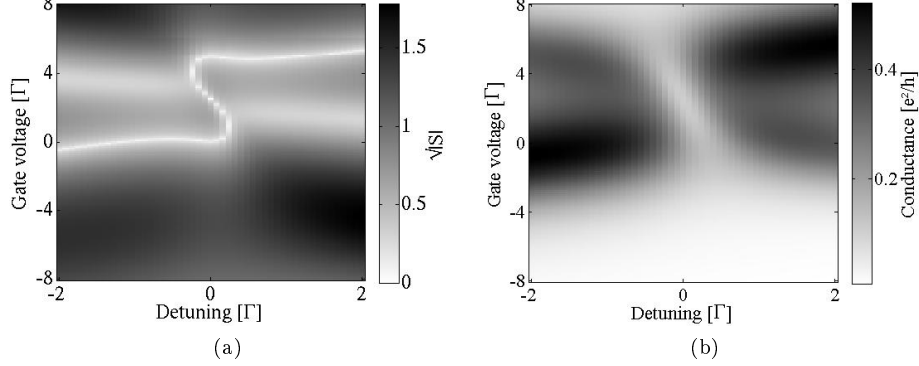
Figure 15: The parameters used were $U = 5\Gamma$, $t_{1L} = t_{1R} = 1$, $t_{2R} = 0.5$, $t_{2L} = -0.5$, $E_{01/02} = 0$ and $g_{1/2} = \pm 1$. **a)** The square root of the absolute value of thermopower at $k_B T = 1.00\Gamma$ and $\triangle k_B T = 0.10\Gamma$. **b)** Conductance at $V = 0.5\Gamma$ and $k_B T = 1.05\Gamma$.

With decreasing U the lines at $V_g = U$ and $V_g = \frac{U}{2}$ come closer to the line at $V_g = 0$. In Fig. 15a with $U = 5\Gamma$, the line at $V_g = \frac{U}{2}$ has merged with $V_g = U$ for negative detuning and with $V_g = 0$ for positive detuning. What remains is only one united zero-thermopower line in an 'S-shape'. Around zero detuning this line follows the canyon of suppression. In these plots, the signal for the canyon of conductance suppression is stronger in the thermopower plot than in the conductance plot. In Fig. 16a and Fig. 16c, one can see that the 'S-shape' flattens out with decreasing U.

With decreasing U, the more strongly coupled level dominates the tunneling more and more. For low enough U , S only changes sign when the more strongly coupled level crosses the Fermi energy. When the weaker coupled level crosses the Fermi energy, the more strongly is closer to the Fermi energy than before and the largest part of tunneling occurs around that energy. In Fig. 15a, the more strongly coupled level always dominates the tunneling except for very low detuning. In Fig. 16a with $U = 2\Gamma$, the weaker coupled level never dominates transport. This is also evident from the conductance plot Fig.16b where there is only one sequiental tunneling area instead of two seperated.
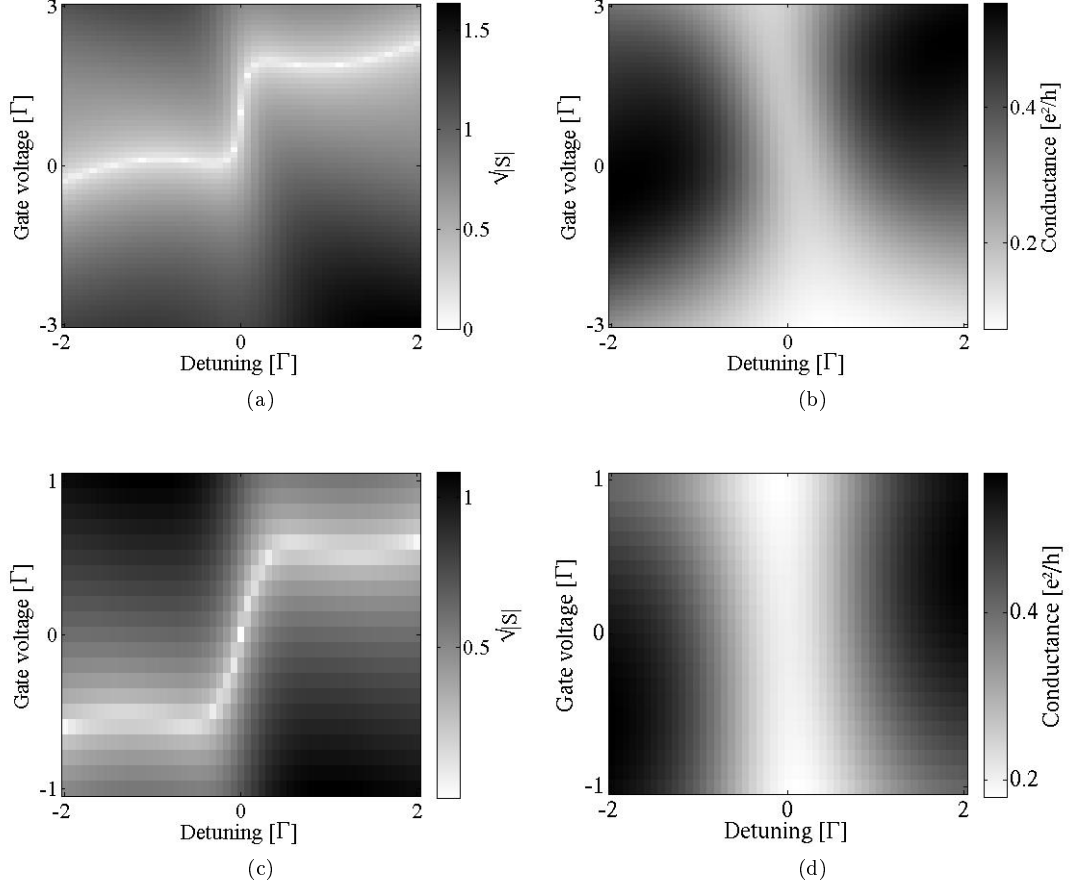
Figure 16: The parameters used were $t_{1L} = t_{1R} = 1$, $t_{2R} = 0.5$, $t_{2L} = -0.5$, $E_{01/02} = 0$ and $g_{1/2} = \pm 1$. **a)** The square root of the absolute value of thermopower at $U = 2\Gamma$, $k_B T = 1.00\Gamma$ and $\triangle k_B T = 0.10\Gamma$ **b)** Conductance at $U = 2\Gamma$, $V = 0.5\Gamma$ and $k_B T = 1.05\Gamma$. **c)** The square root of thermopower at $U = 0\Gamma$, $k_B T = 1.00\Gamma$ and $\triangle k_B T = 0.10\Gamma$ **d)** Conductance at $U = 0\Gamma$, $V = 0.5\Gamma$ and $k_B T = 1.05\Gamma$.

7.4 Highly asymmetric coupling strengths

In the following simulations, the parameters where chosen to perfectly reproduce the conductance results in Ref. [6], along with additional thermopower plots. Here, the energy levels have different magnitudes of the coupling strengths to the right and left lead. In these plots, the energy levels are degenerate at $B = 2\Gamma$.

In the conductance simulations in Fig. 17b and Fig. 17d, one can see from the sequential tunneling lines and the reversed tilting of the canyon, that in contrast to in Sec. 7.3, $\Gamma_2 > \Gamma_1$ instead of the opposite. This can also be seen in the thermopower simulations. In Fig. 17a, the weaker coupled part of the outer line is closer to the middle line than the more strongly coupled part. In Fig. 17c, it is only the more strongly coupled level crossings that remains. As Fig. 17a can be compared to the appearance in Fig. 14a and Fig. 17c can be compared to Fig. 16a one can conclude that in a simulation somewhere between $U = 5\Gamma$ and $U = 2\Gamma$, one would find the S-shape from Fig. 15a, only mirrored.
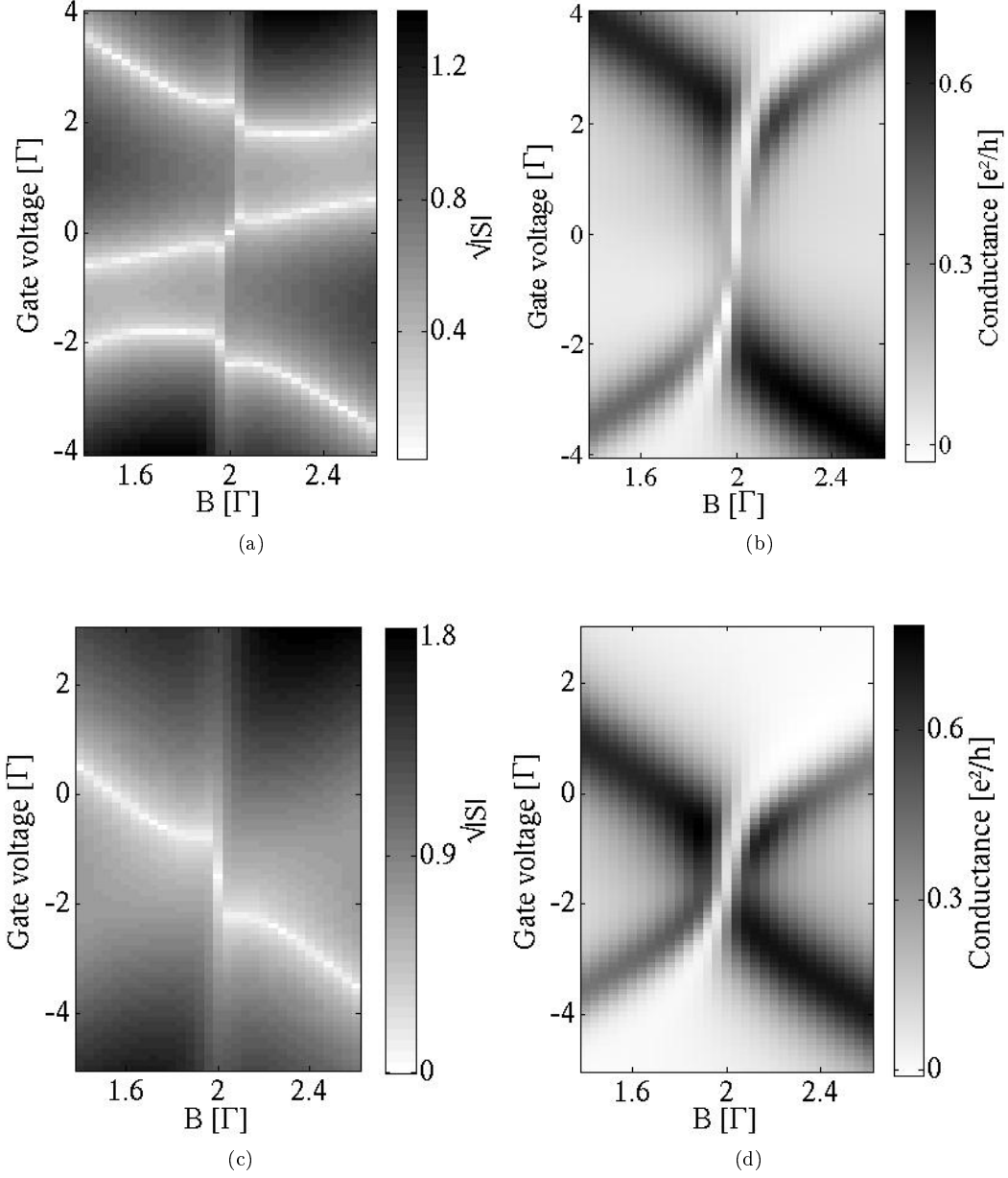
(a)   (b)

(c)   (d)

Figure 17: The parameters used were $t_{1L} = -\sqrt{0.3}$, $t_{1R} = \sqrt{0.1}$, $t_{2R} = \sqrt{0.4}$ and $t_{2L} = 1$, $E_{01} = -6.5$, $E_{02} = 2.5$, $g_1 = 2$ and $g_2 = -2.5$. **a)** The square root of the absolute value of thermopower at $k_B T = 1.00\Gamma$, $\triangle k_B T = 0.10\Gamma$ and $U = 5\Gamma$. **b)** Conductance at $V = 0.5\Gamma$, $k_B T = 0.2\Gamma$ and $U = 5\Gamma$ **c)** The square root of the absolute value of thermopower at $k_B T = 1.00\Gamma$, $\triangle k_B T = 0.10\Gamma$ and $U = 2\Gamma$ **d)** Conductance at $V = 0.5\Gamma$, $k_B T = 0.2\Gamma$ and $U = 2\Gamma$.

37

8   Discussion and outlook

By measuring the two quantities conductance and thermopower of a QD, you use two different ways to probe the system. For G you apply a bias and for S you apply a ΔT. The difference is in the Fermi functions of the leads. In the case of G, the left and right Fermi function have the same shape but different μ. For S, they have the same μ but different shapes. For G, $f_L - f_R$ will only be non-zero around E_F, with maximum at E_F. In the other case, $f_L - f_R$ is zero at E_F and non-zero away from E_F. Therefore, with conductance, you will probe the possibilities for transport at and around the Fermi level. With thermopower you will probe the transport at all energies, where there are electrons in the leads, at the same time.

The sign of the thermopower will tell you if the majority of transport is carried by electrons or holes. If it is carried by electrons it means that it tunnels at energies over E_F, where electrons go from the hot to the cold lead. If it is carried by holes, it goes below E_F and in the opposite direction. In these simulations, S is negative when transport is carried by electrons and positive for holes.

In Sec. 7.2, there is a zero thermopower line around $V_g = \frac{U}{2}$. The corresponding line should appear for all values of U. In Sec. 7.3, there is also a zero thermopower line around $V_g = \frac{U}{2}$ that disappears for values of $U \leq 5.5$. The corresponding line at $V_g = \frac{U}{2}$ in Sec. 7.4, disappears between $2 < U < 5$. This line indicates at what point the singly occupied and doubly occupied state give the same amount of transport. For equal tunneling amplitudes, this line will always be at $V_g = \frac{U}{2}$ but for non equal it is more unpredictable.

In Fig. 15, the thermopower shows a prominent zero-thermopower line in a 'S-shape'. It follows the two strongest sequential tunneling lines in the conductance plot. Where these lines string together it follows the canyon of current suppression. When the zero thermopower line follows the canyon of current suppression, it gives a stronger signal than the conductance.

This prominent signal should not be seen as a coincidence due to the choice of parameters but something generic. The simulations in Sec. 7.4 show that this shape, but mirrored, should appear for some value of U also with those parameters. The shape is mirrored since $\Gamma_2 > \Gamma_1$ instead of the opposite. The S-shape in the thermopower remains to be further studied in a more systematic way. It is still to be verified that the S-shape should appear in all thermopower measurement where the corresponding conductance shows a canyon of current suppression if $a \neq 1$.

References

[1] D. Ferry, S. Goodnick, J. Bird, *Transport in nanostructures* second edition, Cambridge university press, Cambridge, 2009

[2] K. K. Likharev, *Single-Electron Devices and Their Applications*, Proceedings of the IEEE **87**, 606, 1999

[3] P. Michler, *Single Semiconductor Quantum Dots*, Springer, Berlin, 2009

[4] D. Goldhaber-Gordon, H. Shtrikman, D. Mahalu, D. Abusch-Magder, U. Meirav, M. A. Kastner, *Kondo effect in a single-electron transistor*, Nature (London) **391**, 156, 1998

[5] V. Meden, F. Marquardt, *Correlation-Induced Resonances in Transport through Coupled Quantum Dots*, Phys. Rev. Lett. **96**, 146801, 2006

[6] H.A. Nilsson, O. Karlström, M. Larsson, P. Caroff, J.N. Pedersen, P. Samuelsson, A.Wacker, L. -E. Wernersson, H. Q. Xu, *Correlation-induced conductance suppression at level degeneracy in a quantum dot*, Phys. Rev. Lett. **104**, 186804, 2010

[7] Y. Dubi, M. di Ventra, *Colloquium: Heat Flow and thermoelectricity in atomic and molecular junctions*, University of California-San Diego, 2011

[8] G. J. Snyder, E. S. Toberer, *Complex thermoelectric materials*, Nature materials **7**, 105, 2008

[9] N. Nakpathomkun, H. Q. Xu, H. Linke, *Thermoelectric efficiency at maximum power in low-dimensional systems*, Phys. Rev. B **82**, 235428, 2010

[10] J.N. Pedersen, A. Wacker, *Tunneling through nanosystems: Combining broadening with many-particle states*, Phys. Rev. B **72**, 195330, 2005

[11] J. Koch, M. E. Raikh, F. von Oppen, *Pair Tunneling through Single Molecules*, Phys. Rev. **96**, 056803, 2006

[12] L. H. Kristinsdóttir, O. Karlström, J. Bjerlin, J. C. Cremon, P. Schlagheck, A. Wacker, S. M. Reimann, *Total current blockade in an ultracode dipolar quantum wire*, Phys. Rev. Lett. **110**, 085303, 2013

[13] H. -P. Breuer, F. Petruccione, *The theory of open quantum systems*, Oxford university press, Oxford, 2006

[14] J.J. Sakurai, *Modern quantum mechanics* revised edition, Addison Wesley, 1994, (s.178)

[15] J. N. Pedersen, *Tunneling through Nanostructures - Interactions, Interference and Broadening*, Ph.D thesis, Lund university, 2008

[16] X.C. Tong, *Thermoelectric Cooling Through Thermoelectric Materials* chapter 11 in *Advanced Materials for Thermal Management of electronic packaging*, Springer, New York, 2001

[17] W. Hu, F. Bai, X. Gong, X. Zhan , H. Fu, T. Björnholm, *Organic optoelectronics*, Wiley-VCH, Weinheim, 2013 (section 11.2)

[18] O. Karlström, *Effects of coherence and correlations on transport through nanostructures*, Ph.D thesis, Lund university, 2012

[19] T. E. Humphrey, H. Linke, *Reversible thermoelectric nanomaterials*, Phys. Rev. Lett. **94**, 096601, 2005

[20] S. Fahlvik Svensson, A. I. Persson, E. A. Hoffmann, N. Nakpathomkun, H. A. Nilsson, H. Q. Xu, L. Samuelson, H. Linke, *Lineshape of the thermopower of quantum dots*, New Journal of Physics **14**, 033041, 2012

[21] M. Turek, K.A. Matveev, *Cotunneling thermopower of a single electron transistor*, Phys. Rev. B **65**, 115332, 2002

[22] R. S. Whitney, *Most efficient quantum thermoelectric at finite power output*, Phys. Rev. Lett. **112**, 130601, 2014

[23] O. Karlström, H. Linke, G. Karlström, A. Wacker, *Increasing thermoelectric performance using coherent transport*, Phys. Rev. B **84,** 113415, 2011

[24] O. Karlström, J.N. Pedersen, P. Samuelsson, A.Wacker, *Canyon of current suppression in an interactiong two-level quantum dot*, Phys. Rev. B **83,** 205412, 2011